Electronic Supplementary Material (ESI) for Materials Chemistry Frontiers.

Supporting Information For:

A Self-Cleaning Hydrophobic MOF Based Composite for Highly Efficient and Recyclable Separation of Oil from Water and Emulsion

Subhrajyoti Ghosh,[†a] *Abhijeet Rana,*[†a] *Saurav Kumar,*[a] *Chiranjib Gogoi,*[a] *Srijan Mukherjee,*[a] *Uttam Manna*[a] *and Shyam Biswas**[a]

[a] Department of Chemistry, Indian Institute of Technology Guwahati, Guwahati, 781039 Assam, India.

[†]*Both are first authors*

* Corresponding author. Tel: 91-3612583309, Fax: 91-3612582349.

E-mail address: sbiswas@iitg.ac.in

Materials and General Methods:

All the reagents and solvents were purchased from commercial sources and used without purification, except the 2-hydroxyterephthalic acid (H_2BDC-OH) linker which was prepared according to the reported procedure.[1] The melamine sponge was purchased from Amazon India. The Attenuated Total Reflectance Infrared (ATR-IR) spectra were recorded using PerkinElmer UATR Two at the ambient condition in the region 400-4000 cm^{-1}. The notations used for characterization of the bands are broad (br), strong (s), very strong (vs), medium (m), weak (w) and shoulder (sh). Thermogravimetric analysis (TGA) was carried out with a Netzsch STA-409CD thermal analyzer in the temperature range of 25-700 °C in an air atmosphere at the rate of 10 °C min^{-1}. Bruker D2 Phaser X-ray diffractometer was employed for powder X-ray diffraction (PXRD) measurements at 30 kV, 10 mA using Cu-$K\alpha$ (λ = 1.5406 Å) radiation. N_2 sorption isotherms were recorded by using Quantachrome Quadrasorb evo volumetric gas adsorption equipment at −196 °C. Before the sorption analysis, the degassing of the compound was carried out at 120 °C under a high vacuum for 12 h. Pawley refinement was carried out using Materials Studio software. The DICVOL program incorporated within STOE's WinXPow software package was used to determine the lattice parameters. The contact angle measurements were performed by employing a KRUSS Drop Shape Analyzer-DSA-25 instrument with an automatic liquid dispenser at ambient temperature.

Measurement of Absorption Capacities for Various Oils by 1′@CF_3@melamine Composite:

For the oil absorption measurement, fully dry pre-weighed (~300-400 mg) **1′@CF_3@melamine** composite was placed in various heavy oils ($CHCl_3$, CH_2Cl_2 and CCl_4) and light oils (hexane, EtOAc, toluene, motor oil, gasoline and kerosene). The composites were kept in oil for 1 min to reach absorption equilibrium and then removed and weighed. All the experiments were performed at room temperature. Absorption capacities for various oils were calculated using the following formula:

Absorption capacity (g/g) = $(W_f-W_i)/W_i$

Where, W_i was the initial weight of **1′@CF_3@melamine** composite and W_f was the weight of oil-absorbed **1′@CF_3@melamine**. Six measurements were performed for each oil sample and the average value was plotted.

Absorption Based Separation of Oil and Water by 1′@CF_3@Melamine Composite:

A single piece of dry pre-weighed **1′@CF_3@melamine** composite (300-400 mg) was placed in several oil/water combinations containing 3 mL of oil and 40 mL of water to separate the light oils (hexane, EtOAc, toluene, motor oil, gasoline and kerosene) from the surface of the water. For heavy oils (CH_2Cl_2, $CHCl_3$ and CCl_4), a piece of **1′@CF_3@melamine** composite was brought into contact with the sediment oil for the separation of heavy oils from the oil/water combination from the bottom of the water. For each case, the **1′@CF_3@melamine** composite selectively soaked the oils when it came with the contact of oils and the separated oil was recovered by physically squeezing the material. All the tests were performed at room temperature. Separation efficiency (%) for various oils were calculated using the following formula:

Separation efficiency (%) = V_f/V_i x 100%

where V_i was the amount of oil used (mL) and V_f was the absorbed volume of water (mL). Six measurements were performed for each oil sample and average value was plotted.

Separation of Emulsions Using 1′@CF$_3$@Melamine Composite:

All the water-in-oil emulsions were prepared (water/toluene, water/$CHCl_3$, water/ kerosene and water/gasoline) by sonicating the water-oil mixtures for 60 min. To make the emulsion stable, 50 μL of surfactant (Triton X-100) was added to the oil-water mixture before sonication. Then, 4 mL (3.5 mL of oils + 0.5 mL of water) of different water-in-oil emulsions were allow to pass through a chromatographic column and the bottom of the column was packed by hydrophobic **1′@CF$_3$@Melamine** composite. The time required for all the separation process were recorded.

Separation efficiency (%) for various water-in-oil emulsion were calculated using the following formula:

Separation efficiency (%) = $V_2/V_1 \times 100\%$

where V_1 is the amount of oil used (mL) for the preparation of the water-in-oil emulsion and V_2 is the obtained volume of oil (mL) after the separation experiment.

The flux for various emulsions were calculated using the formula: Flux = $V/A \times T$ (where V = volume of separated oil, A = area of the composite and T = time required for the separation of oil from water-in-oil emulsion).

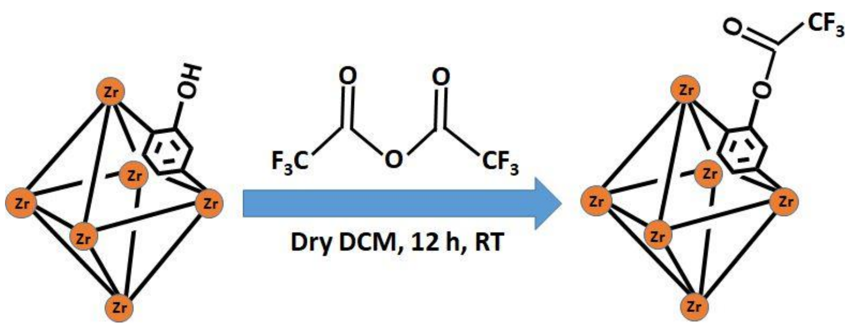

Scheme S1. Reaction scheme for the preparation of **1′@CF$_3$** MOF.

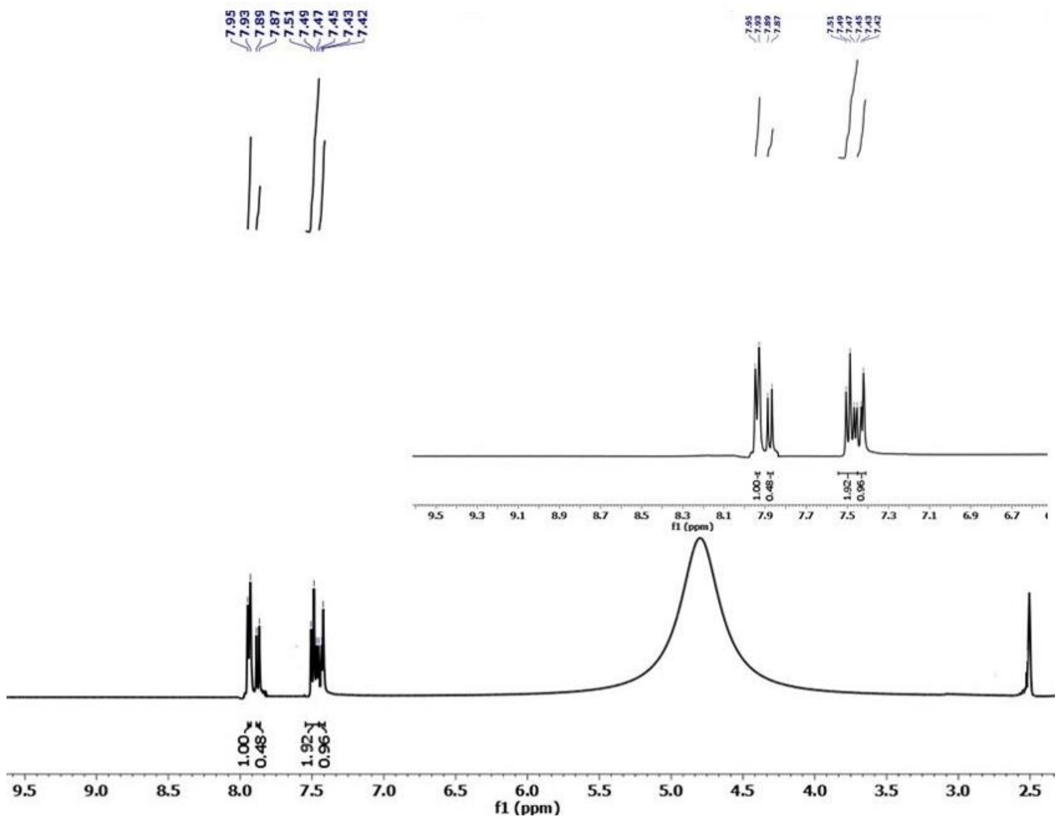

Figure S1. [1]H NMR spectrum of the digested **1′@CF$_3$** MOF in DMSO-d$_6$. The MOF was digested after adding two drops of 40% HF in DMSO-d$_6$ medium.

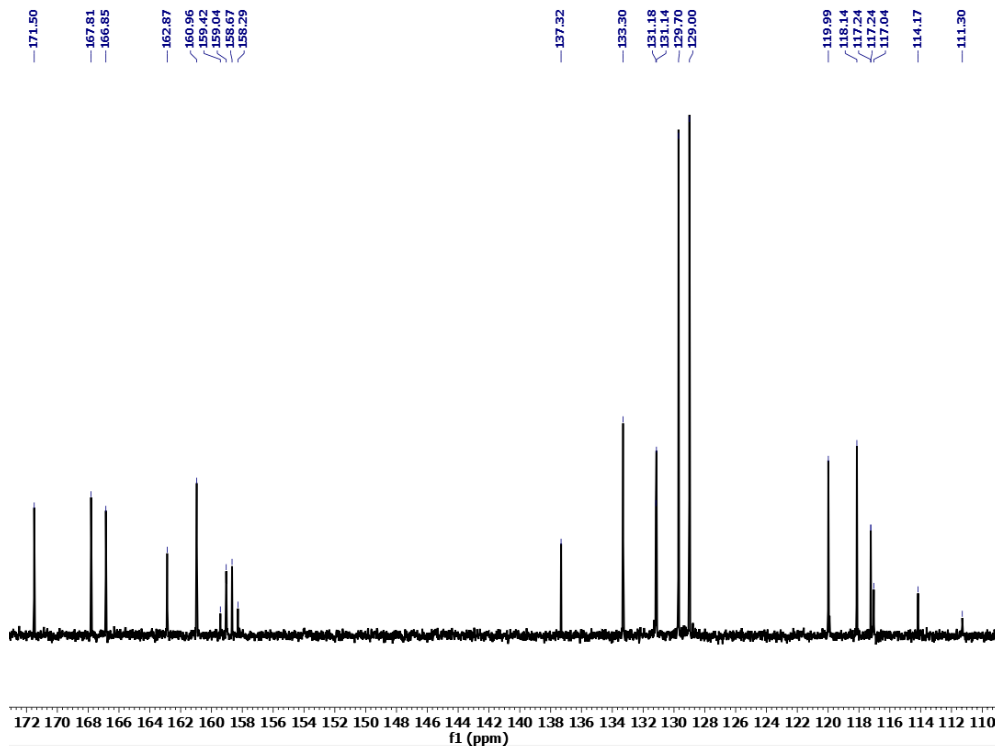

Figure S2. [13]C NMR spectrum of the digested **1′@CF$_3$** MOF in DMSO-d$_6$. The MOF was digested after adding two drops of 40% HF in DMSO-d$_6$ medium.

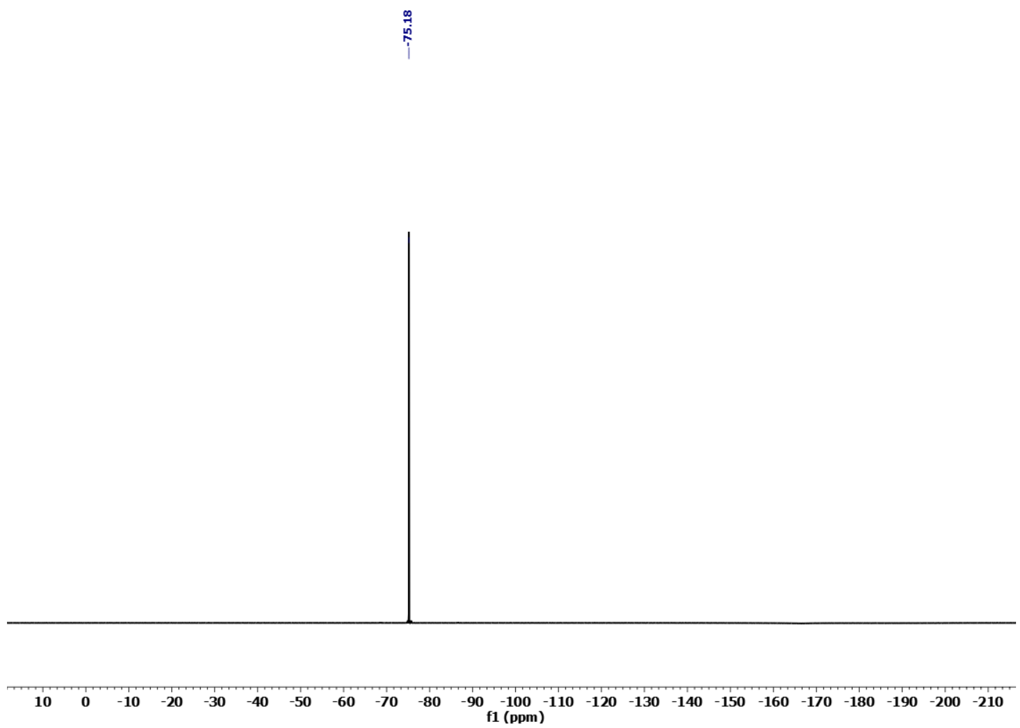

Figure S3. [19]F NMR spectrum of the digested **1′@CF$_3$** MOF in DMSO-d$_6$. The MOF was digested after adding two drops of 40% HF in DMSO-d$_6$ medium.

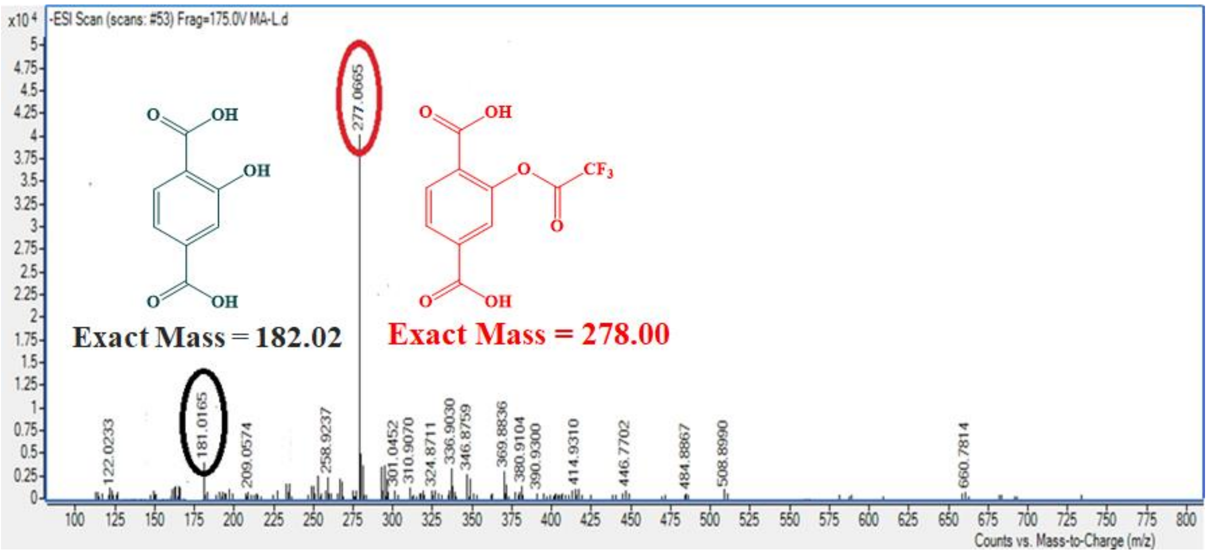

Figure S4. ESI-MS spectrum of **1′@CF$_3$** MOF measured in methanol. The spectrum shows m/z peak at 277.0665, which corresponds to (M-H)$^-$ ion (M = mass of H$_2$BDC-OCOCF$_3$ linker) and m/z peak at 181.0165 corresponds to (M-H)$^-$ ion (M = mass of H$_2$BDC-OH linker).

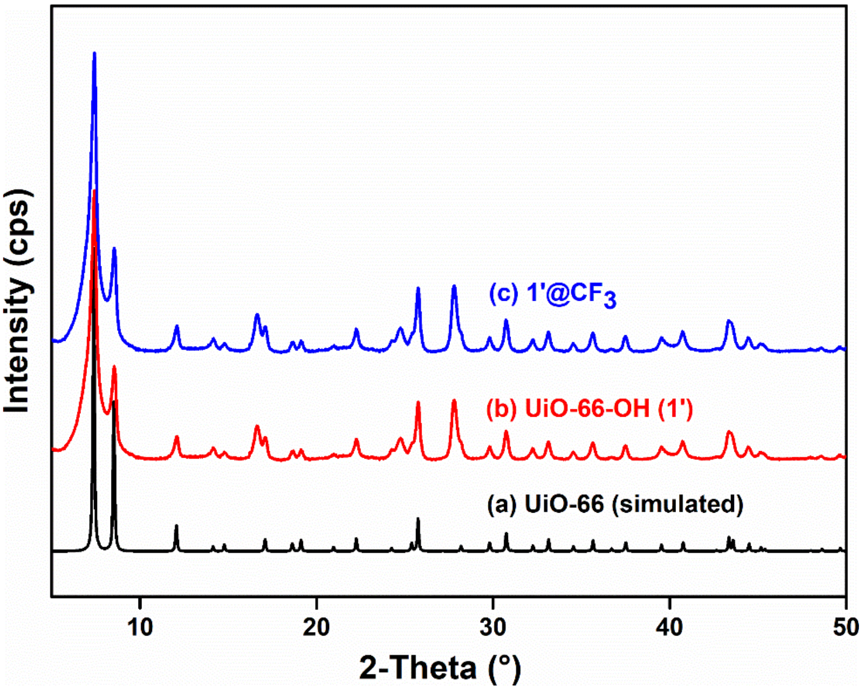

Figure S5. PXRD patterns of (a) Zr-UiO-66 (black), (b) activated Zr-UiO-66-OH (red) and (c) **1′@CF₃** (blue).

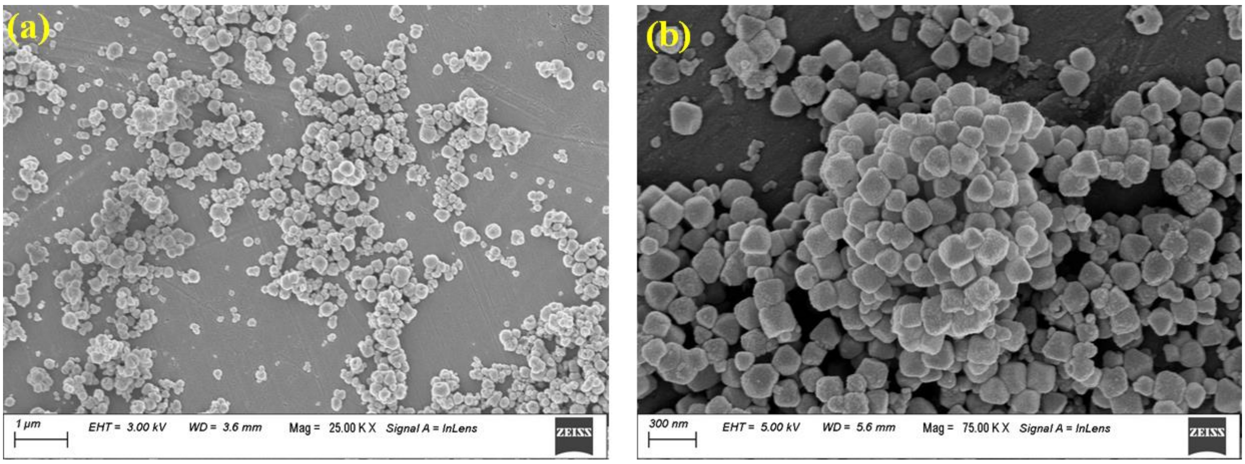

Figure S6. FE-SEM images of (a) **1′** and (b) **1′@CF₃**.

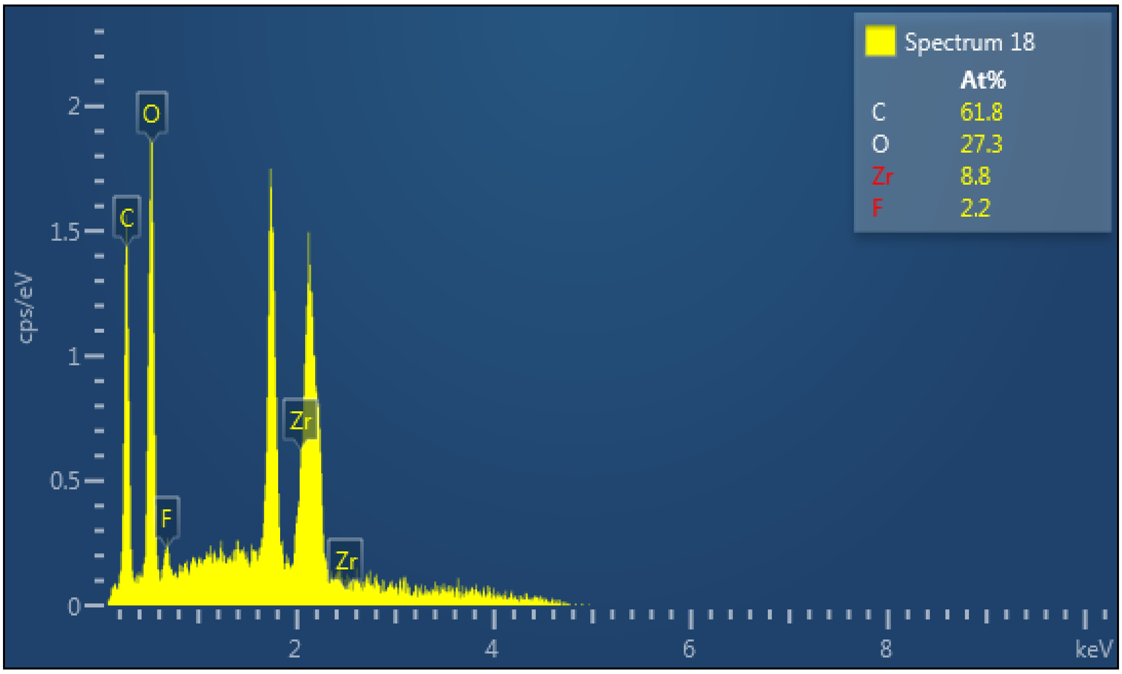

Figure S7. EDX spectrum of **1′@CF$_3$**.

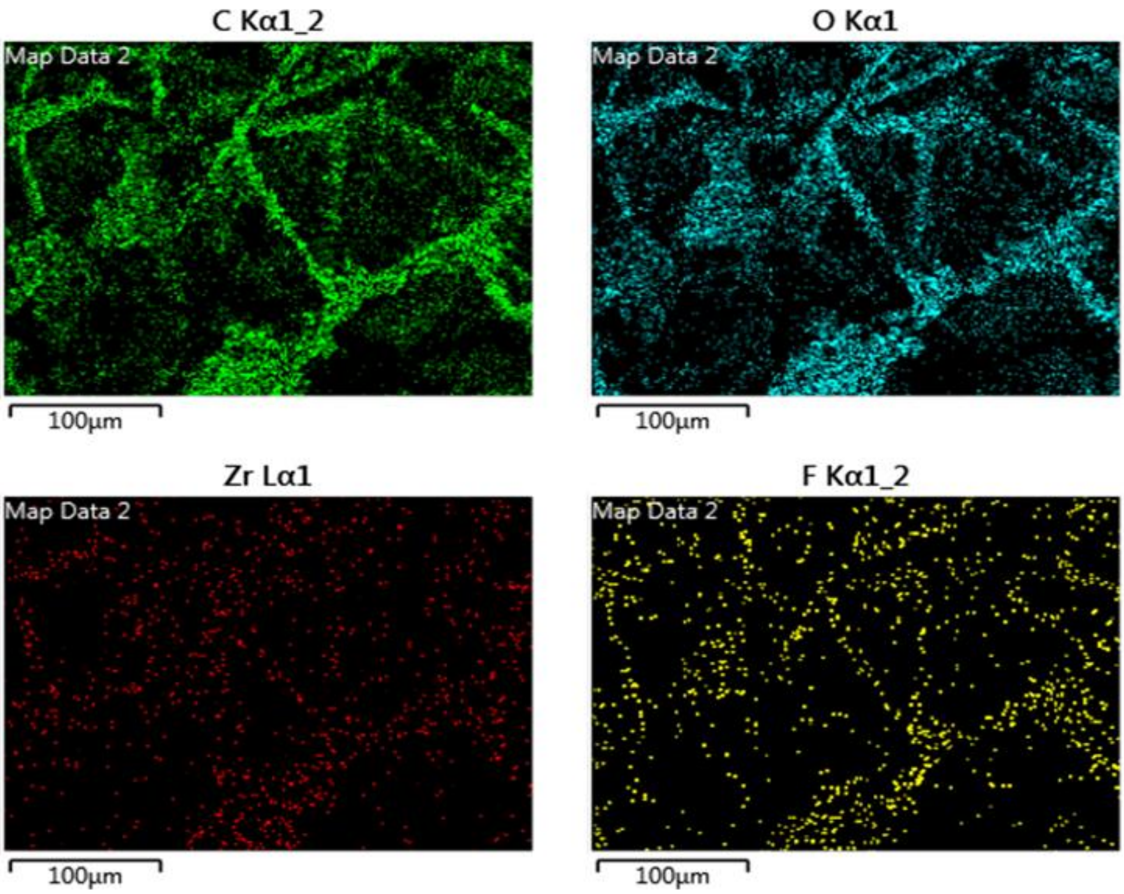

Figure S8. EDX elemental mapping of **1′@CF$_3$**.

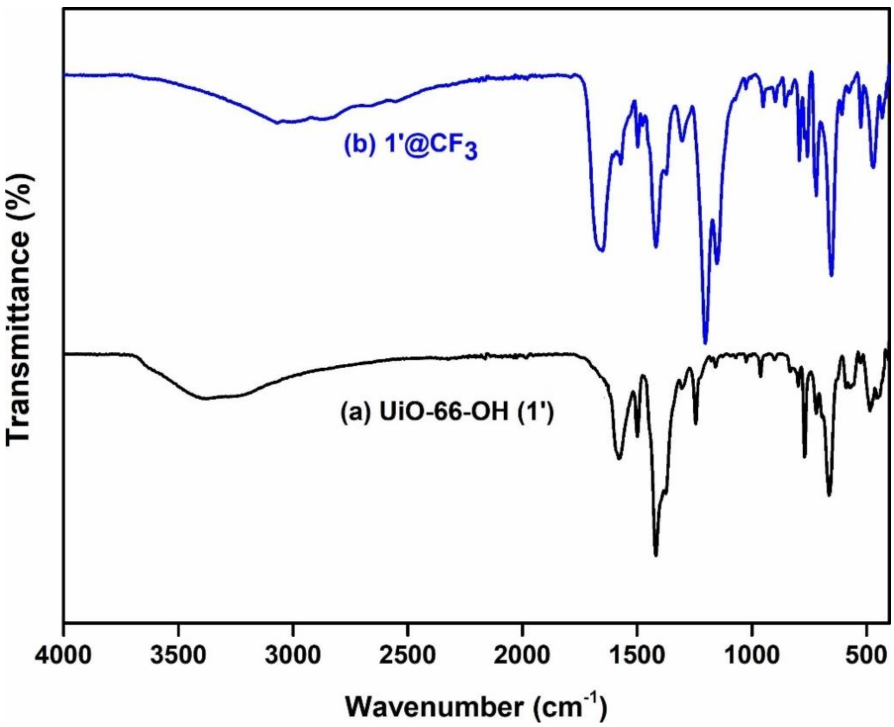

Figure S9. FT-IR spectra of (a) **UiO-66-OH** (**1′**) and (b) **1′@CF$_3$** MOF.

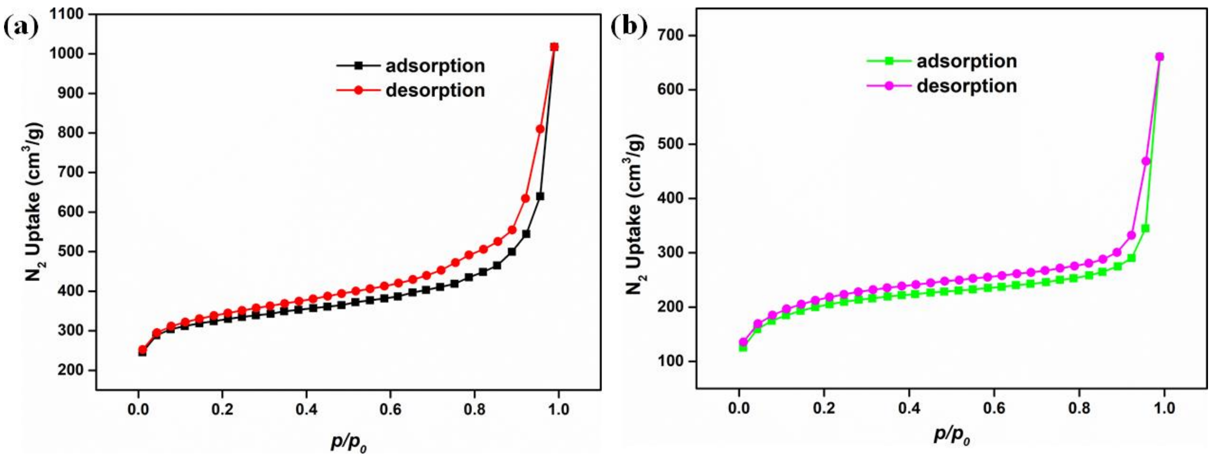

Figure S10. Nitrogen adsorption and desorption isotherms of (a) **1'** and (b) **1′@CF$_3$** recorded at –196 °C.

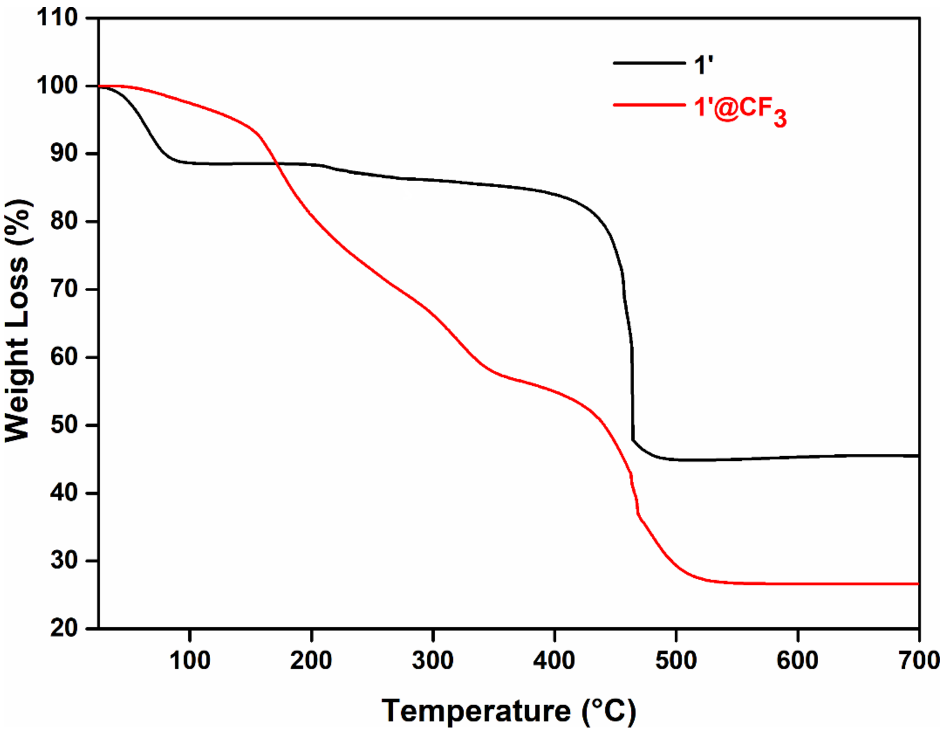

Figure S11. TGA curves of activated **1'** (black) and (b) **1′@CF$_3$** (red) recorded in an air atmosphere in the temperature range of 25-700 °C at a heating rate of 10 °C min^{-1}.

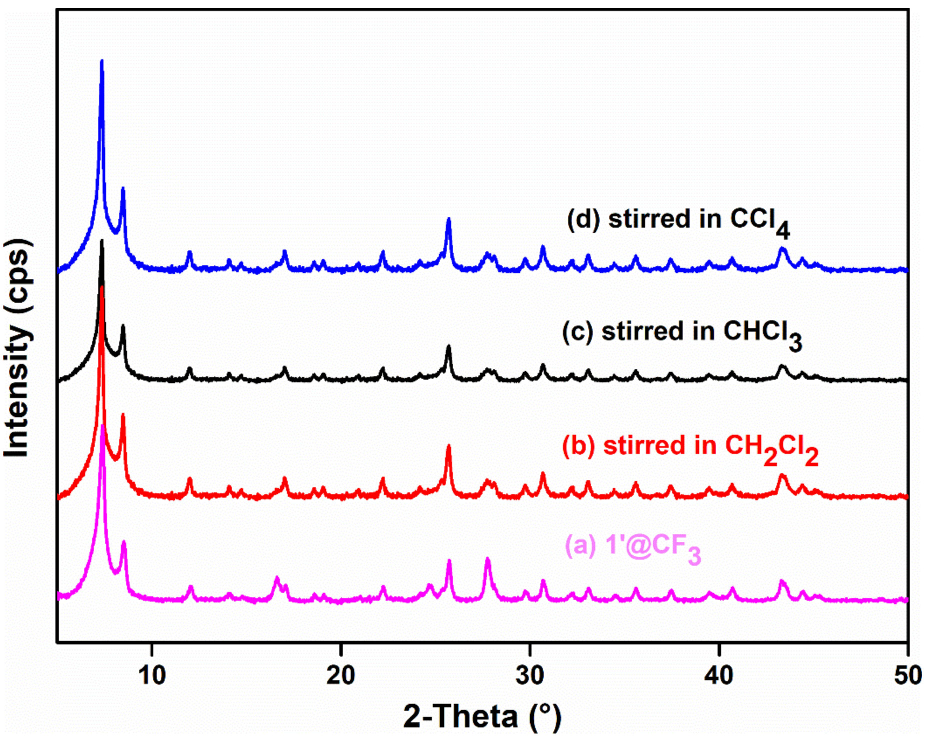

Figure S12. PXRD patterns of (a) **1′@CF$_3$**, **1′@CF$_3$** after stirring in (b) CH_2Cl_2, (c) $CHCl_3$ and (d) CCl_4.

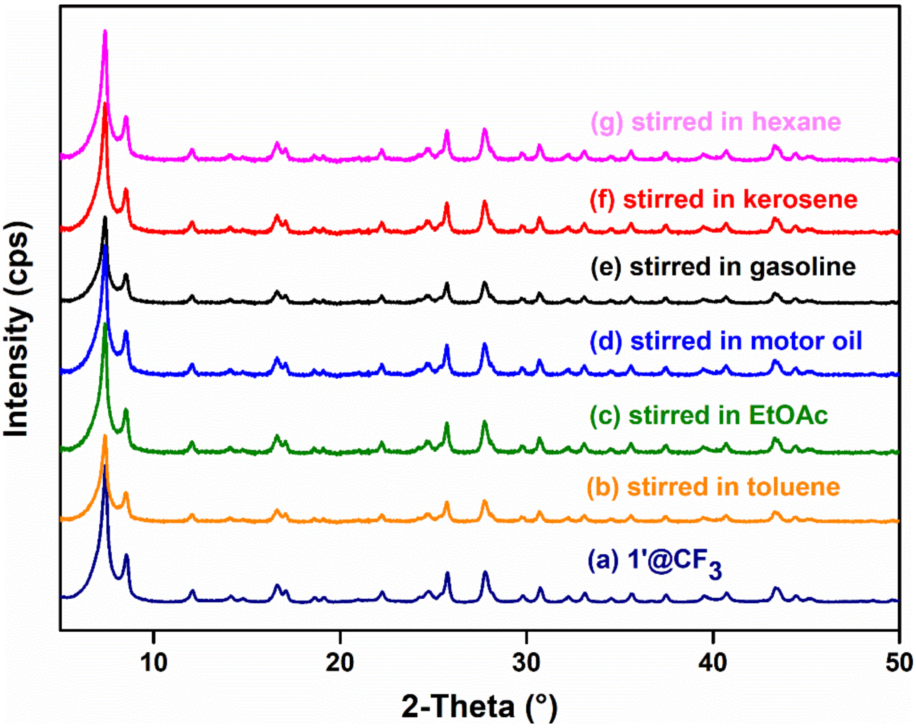

Figure S13. PXRD patterns of (a) **1′@CF₃**, **1′@CF₃** after stirring in (b) toluene, (c) EtOAc, (d) motor oil, (e) gasoline, (f) kerosene and (g) hexane for 24 h.

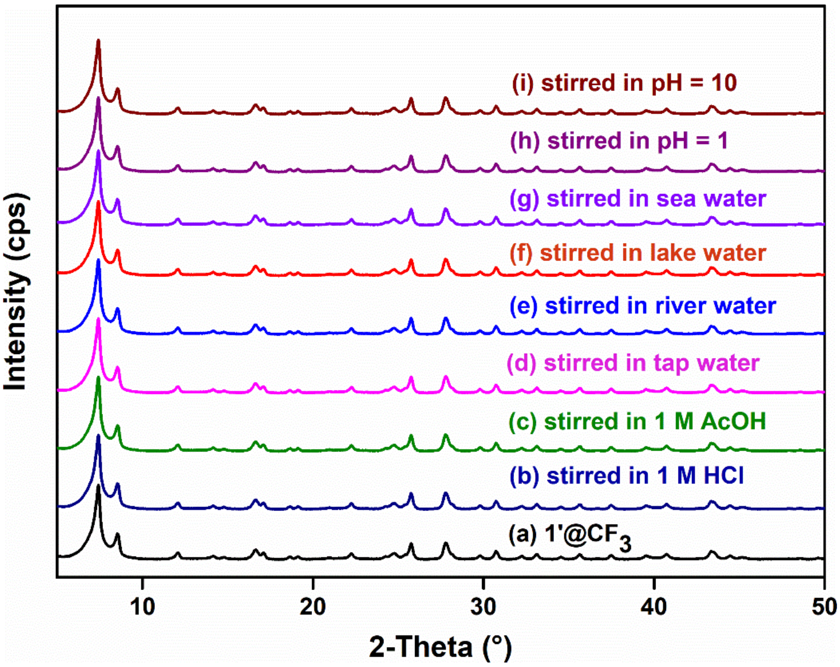

Figure S14. PXRD patterns of (a) **1′@CF₃**, **1′@CF₃** after stirring in (b) 1 M HCl, (c) 1 M AcOH, (d) tap water, (e) river water, (f) lake water, (g) sea water, (h) pH = 1 and (i) pH = 10 for 24 h.

Table S1. Water Contact angle (WCA) of **1′@CF₃** after treatment with different types of water and oil specimens.

Liquids	Average WCA of **1′@CF₃** (°)

Fresh **1′@CF$_3$**	146 ± 1.0
CCl_4	144 ± 1.2
$CHCl_3$	146 ± 1.5
CH_2Cl_2	143 ± 1.3
Hexane	142 ± 1.2
kerosene	143 ± 1.1
Gasoline	142 ± 1.3
Motor oil	140 ± 1.6
EtOAc	141 ± 1.1
Toluene	146 ± 1.2
pH =1	142 ± 1.6
pH = 10	146 ± 1.4
Sea water	141 ± 1.0
Lake water	143 ± 1.5
Tap water	145 ± 1.3
River water	143 ± 1.2
1 M AcOH	142 ± 1.0
1 M HCl	144 ± 1.0

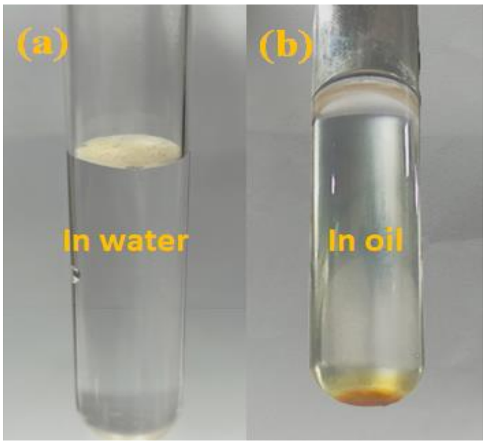

Figure S15. Self-floating ability of **1′@CF$_3$** in water (a) and oil (hexane) (b).

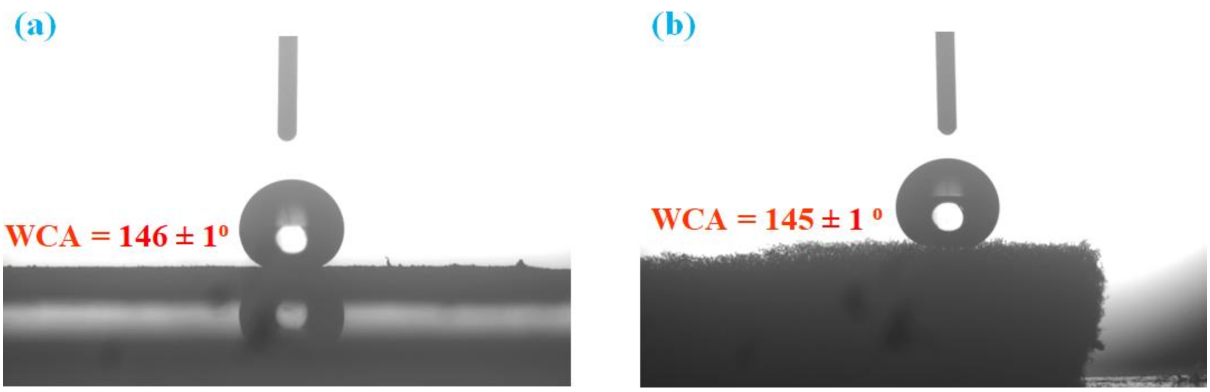

Figure S16. The contact angle image of beaded water droplets on the surface of (a) **1′@CF$_3$** and (b) **1′@CF$_3$@melamine** composite.

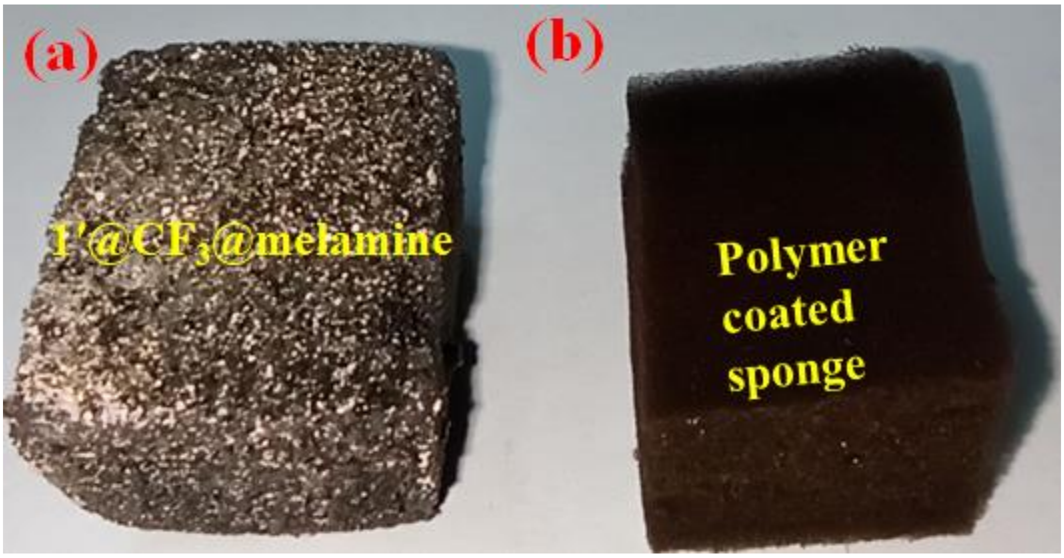

Figure S17. Digital images of (a) **1′@CF$_3$@melamine** composite and (b) polymer coated melamine sponge.

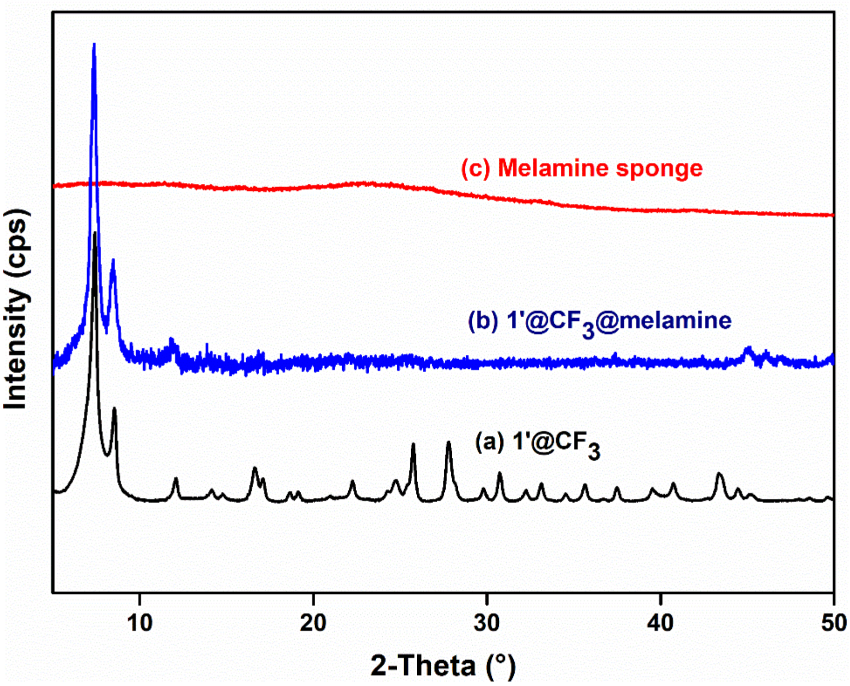

Figure S18. PXRD patterns of (a) **1′@CF$_3$**, (b) **1′@CF$_3$@melamine** composite and (c) only melamine sponge.

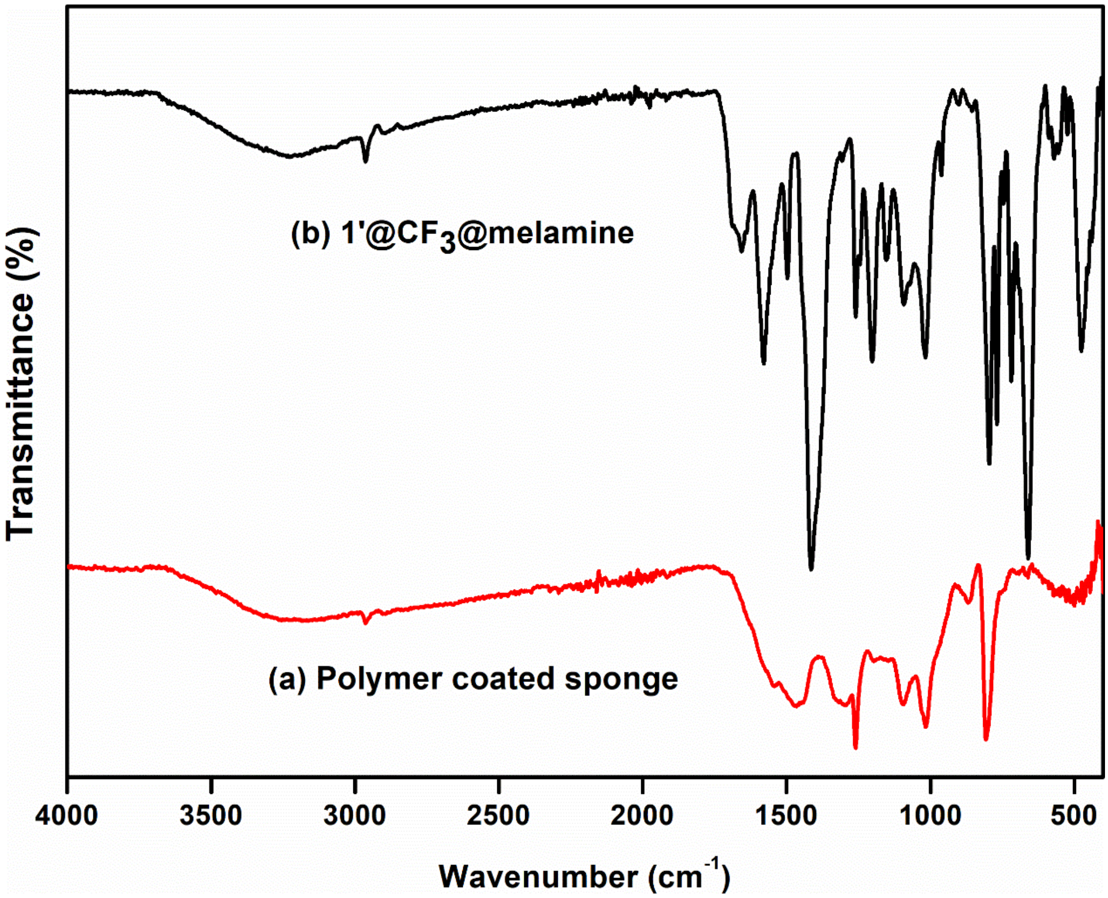

Figure S19. FT-IR spectra of (a) native melamine sponge and (b) **1′@CF_3@melamine** composite.

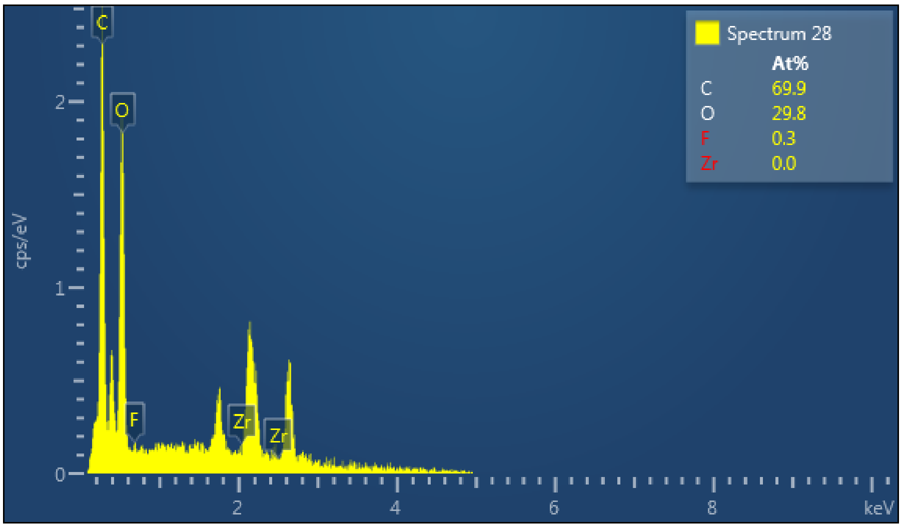

Figure S20. EDX spectrum of melamine sponge.

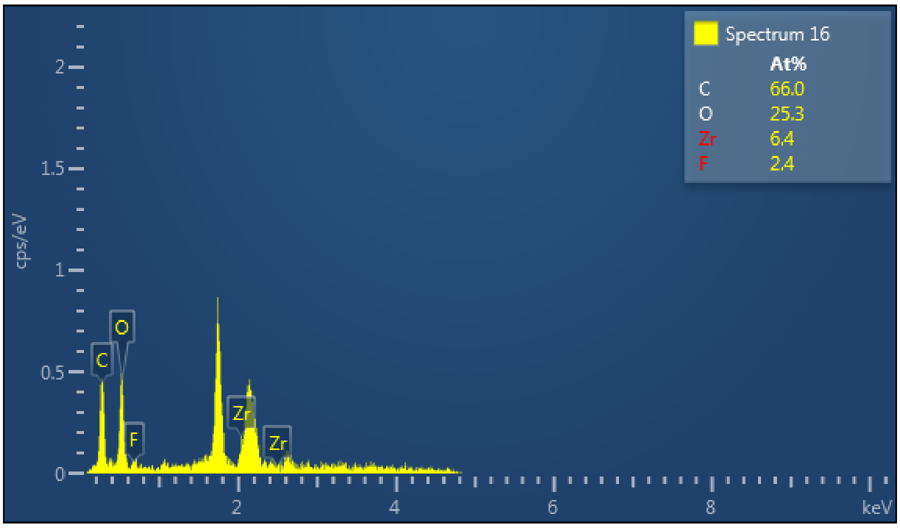

Figure S21. EDX spectrum of **1′@CF_3@melamine** composite.

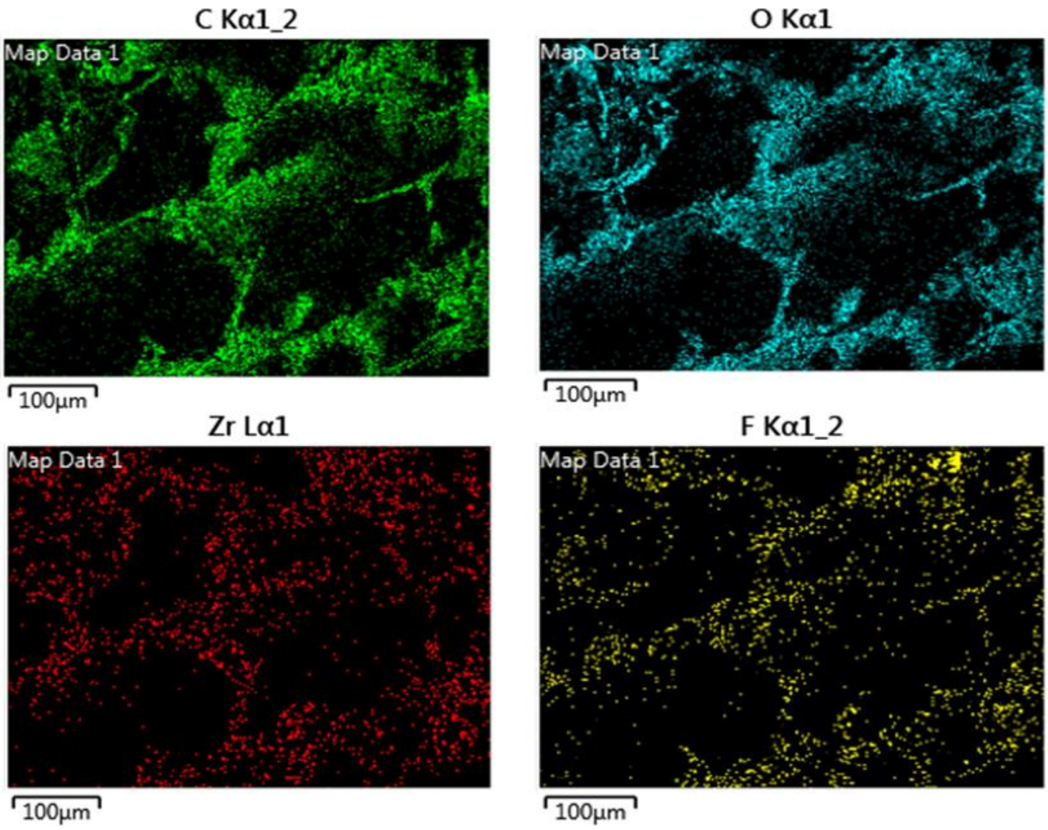

Figure S22. EDX elemental mapping of **1′@CF_3@melamine** composite.

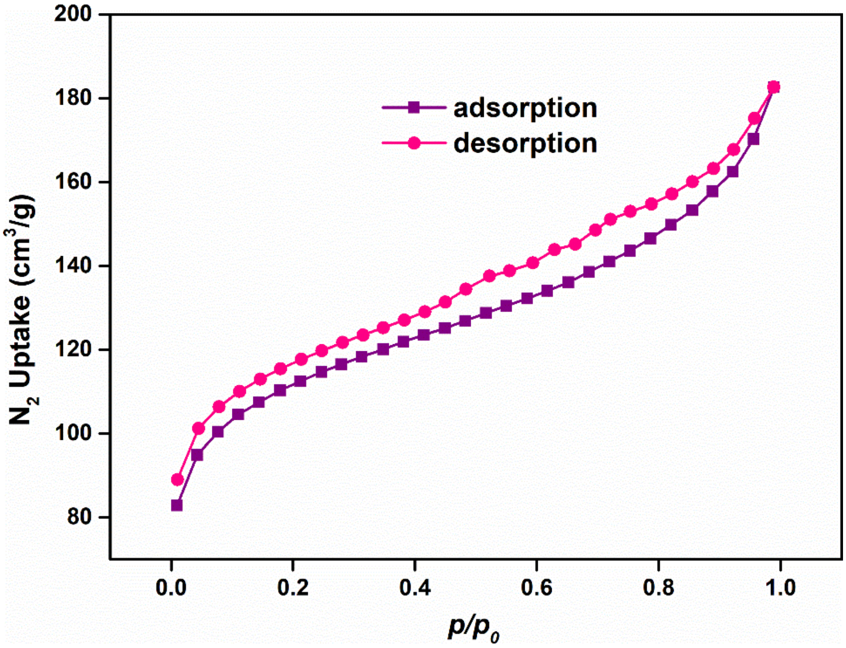

Figure S23. Nitrogen adsorption and desorption isotherms of **1′@CF$_3$@melamine** recorded at -196 °C.

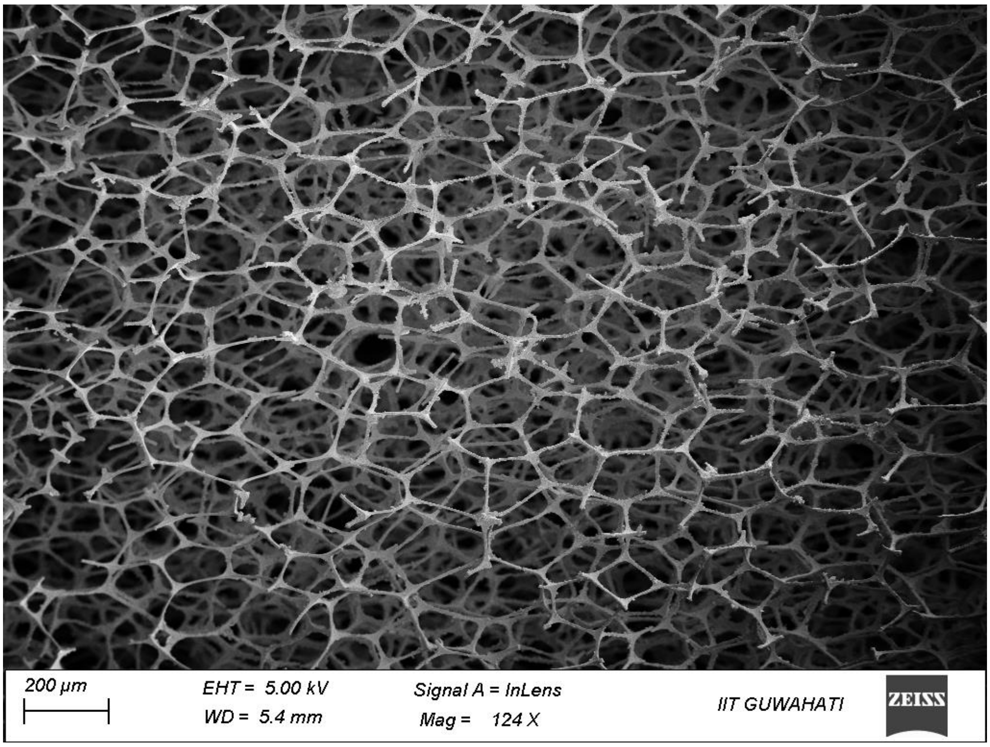

Figure S24. High resolution FE-SEM images of melamine sponge.

Figure S25. Digital images of floating **1′@CF$_3$@melamine** composite on water and immersion of polymer coated melamine sponge in water.

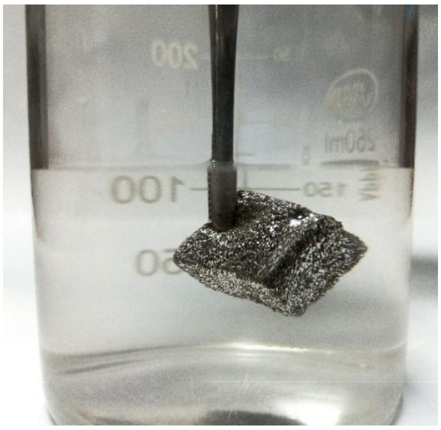

Figure S26. Digital image of forcefully submerged **1′@CF$_3$@melamine** composite under water showed Cassie-Baxter state.

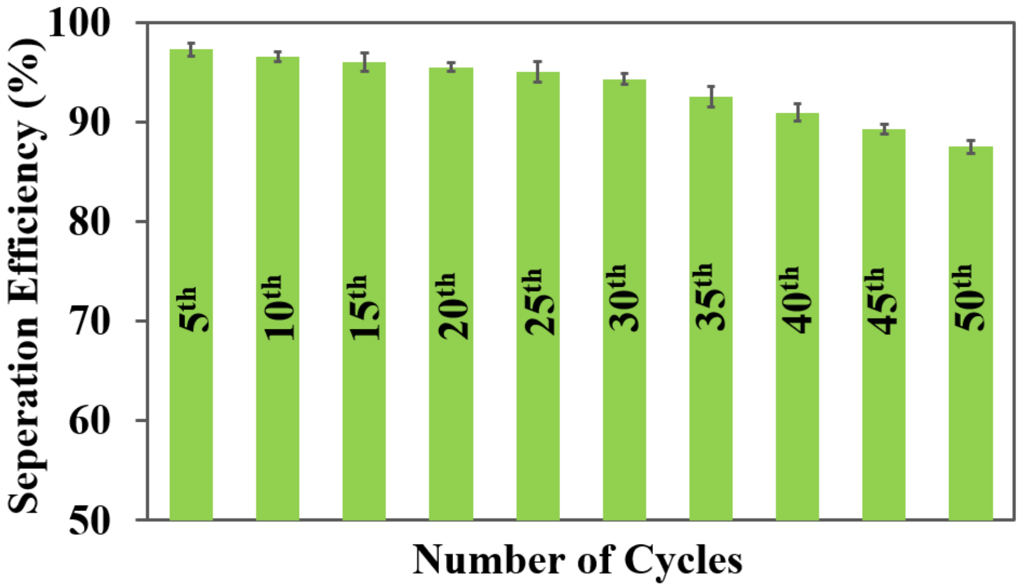

Figure S27. Reusabiity of **1′@CF$_3$@melamine** composite for oil/water separation experiment (model oil: EtOAc).

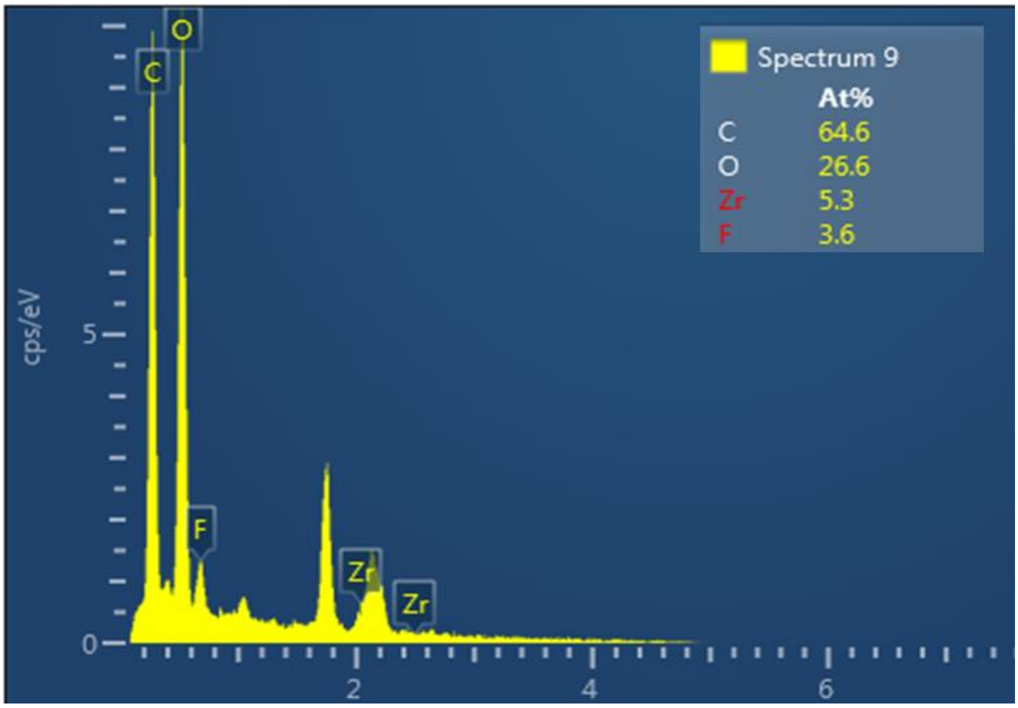

Figure S28. EDX spectrum of **1′@CF$_3$@melamine** composite after 50th cycle of oil-water separation experiment.

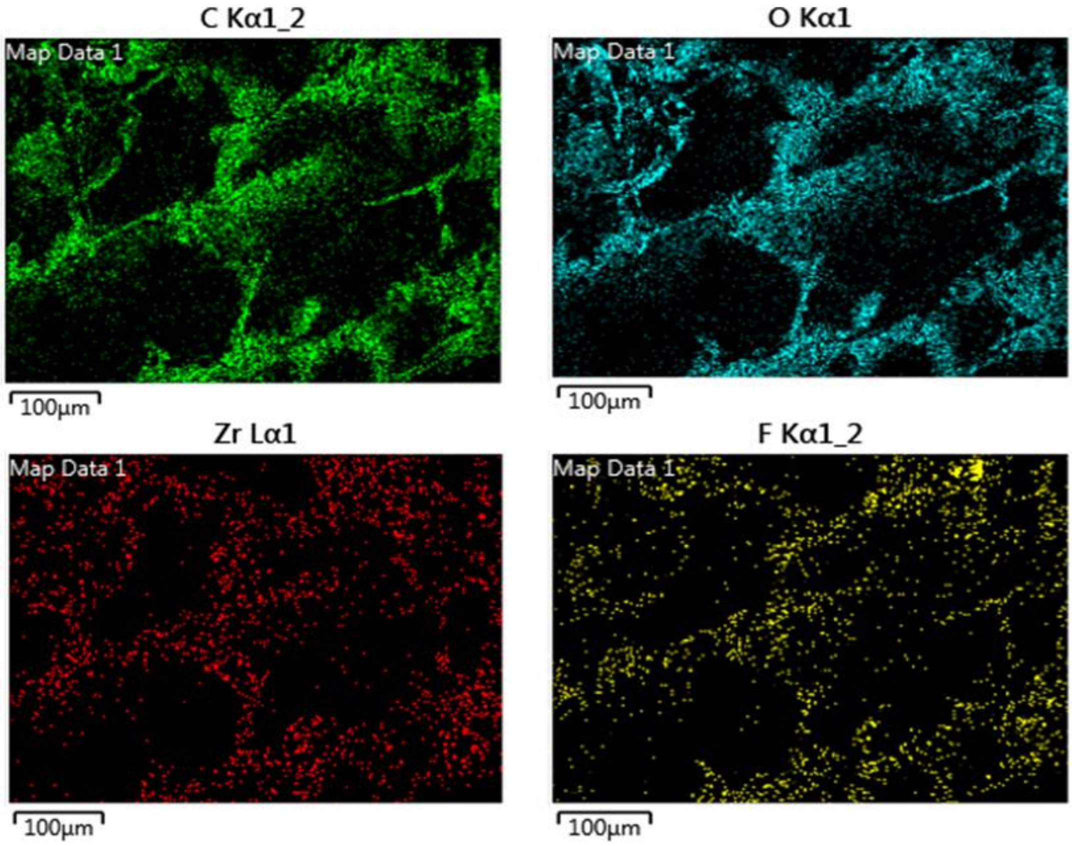

Figure S29. EDX elemental mapping of **1′@CF$_3$@melamine** composite after 50th cycle of oil-water separation experiment.

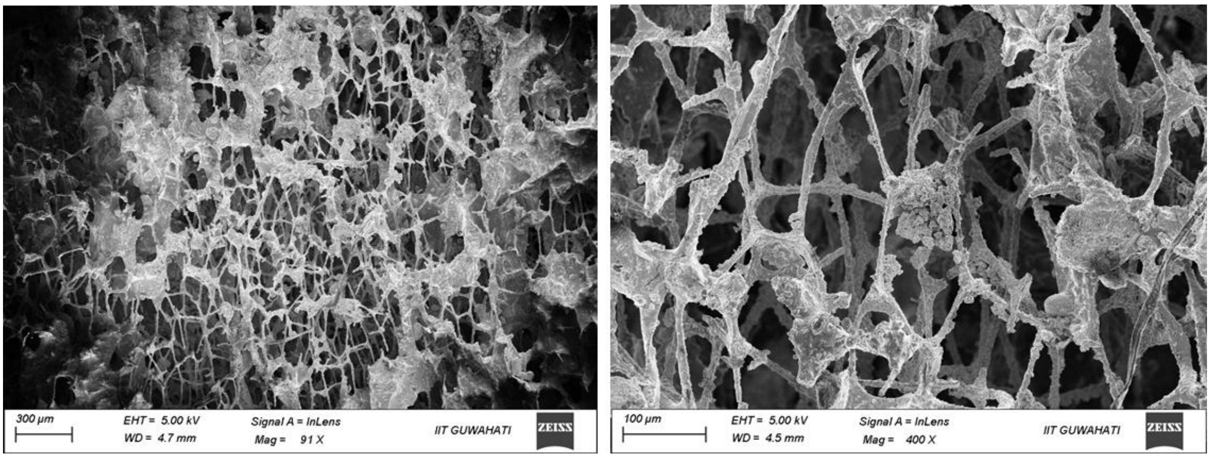

Figure S30. High resolution FE-SEM images of **1′@CF$_3$@melamine** composite after 50th cycle of oil-water separation experiment.

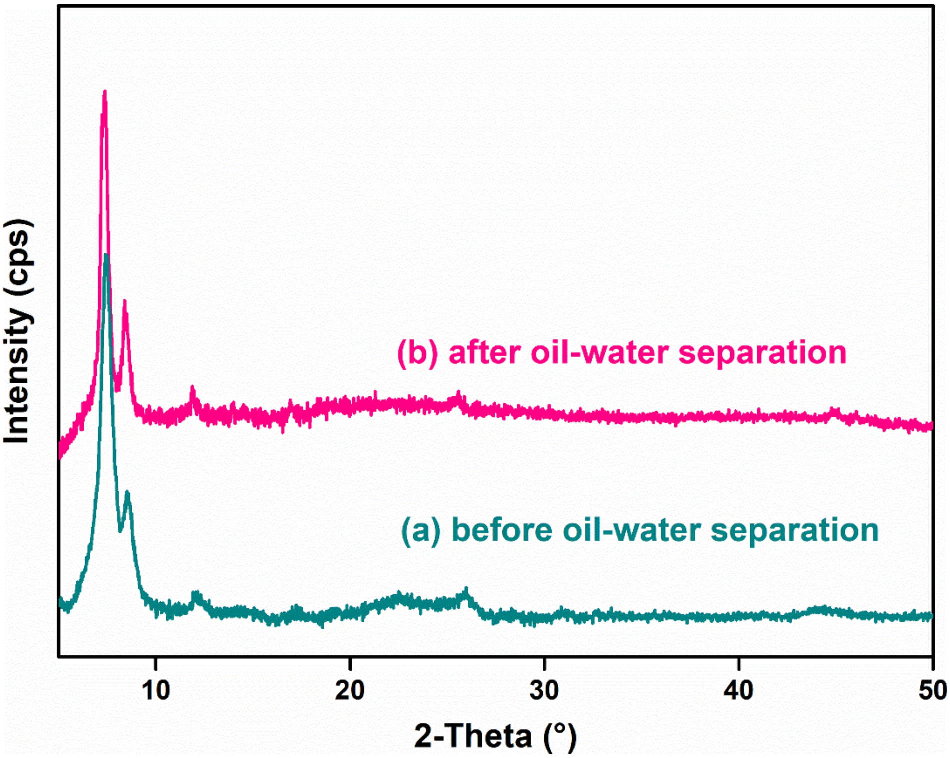

Figure S31. PXRD patterns of **1′@CF$_3$@melamine** composite (a) before and (b) after oil-water separation experiments (model oil: EtOAc).

Table S2. Water Contact angle (WCA) of **1′@CF$_3$@melamine** after treatment with different types of water and oil specimens.

Oil/Water types	Average WCA (°)
Sea water	142 ± 1.8
Lake water	142 ± 1.5
Tap water	143 ± 1.9
River water	144 ± 1.7
Hot water	140 ± 1.9
Cold water	143 ± 1.2
pH = 1	143 ± 2.0
pH = 10	144 ± 1.9
CH_2Cl_2	140 ± 1.1
$CHCl_3$	144 ± 1.2
CCl_4	141 ± 1.3
EtOAc	144 ± 1.5
Hexane	145 ± 1.8
Toluene	142 ± 1.0
Motor oil	147 ± 1.0
Gasoline	147 ± 1.2
Kerosene	145 ± 1.3

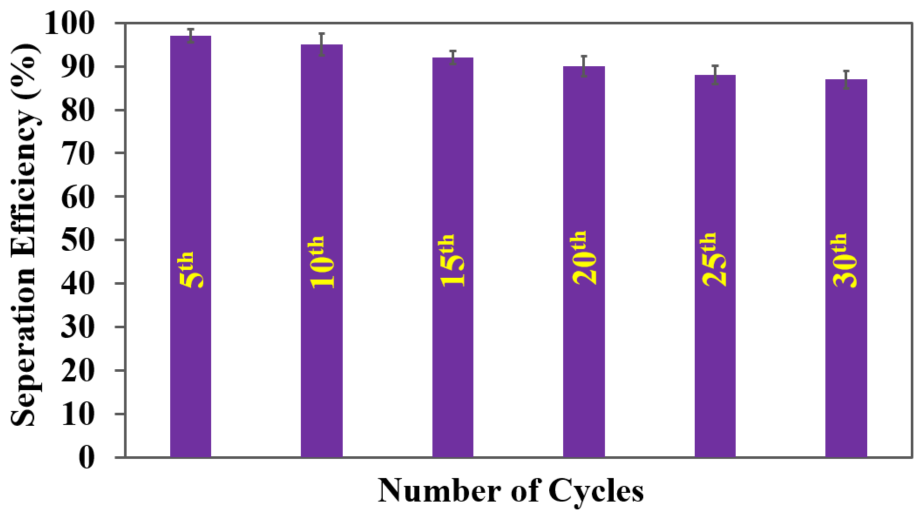

Figure S32. Reusabiity of **1′@CF$_3$@melamine** composite for emulsion separation experiment (model oil: kerosene).

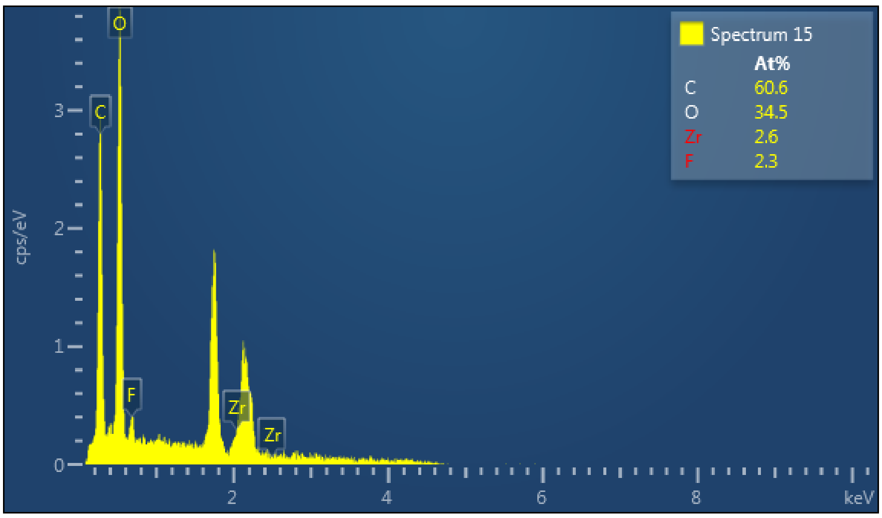

Figure S33. EDX spectrum of **1′@CF$_3$@melamine** composite after 30th cycle of emulsion separation experiment.

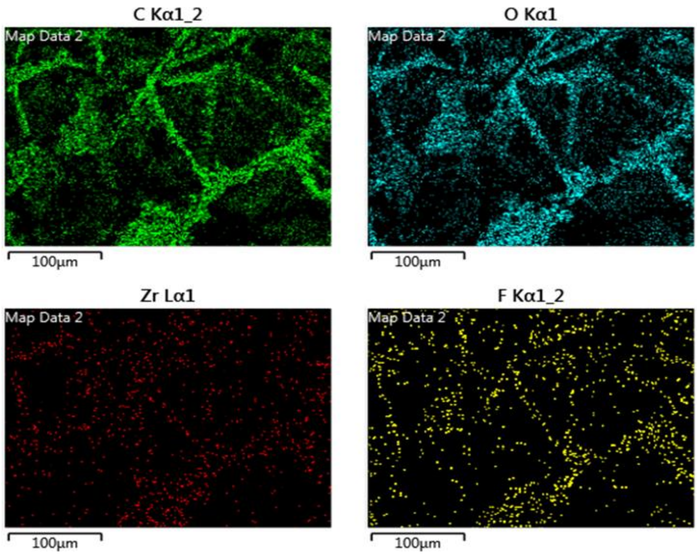

Figure S34. EDX elemental mapping of **1′@CF$_3$@melamine** composite after 30th cycle of emulsion separation experiment.

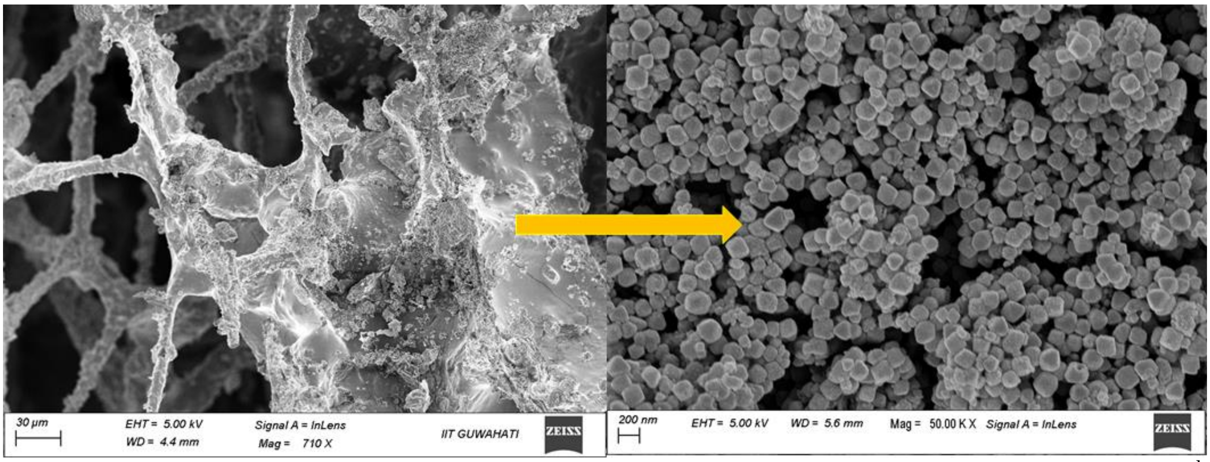

Figure S35. High resolution FE-SEM images of **1′@CF$_3$@melamine** composite after 30th cycle of emulsion separation experiment.

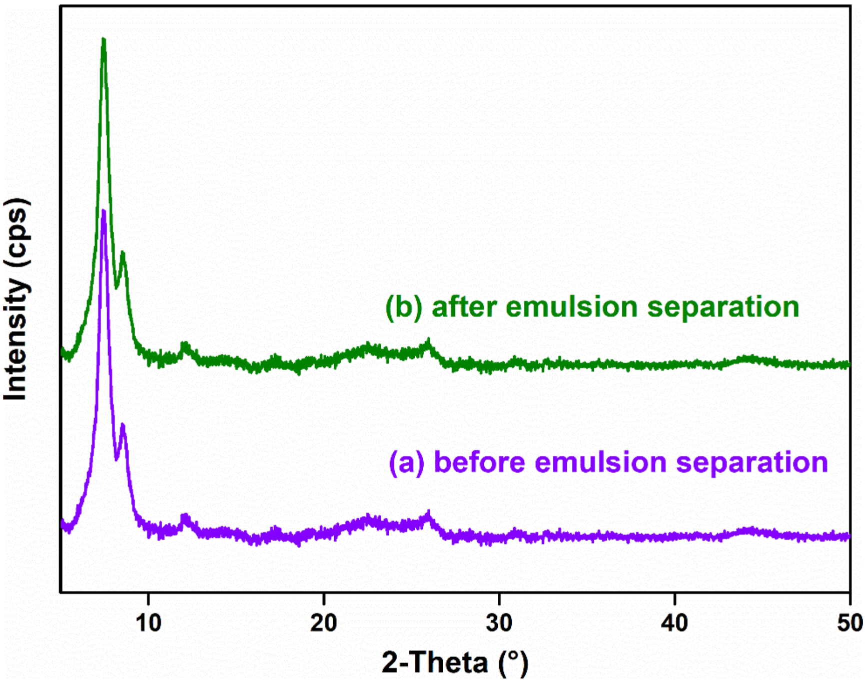

Figure S36. PXRD patterns of **1′@CF$_3$@melamine** composite before and after emulsion separation experiments (model oil: kerosene).

Table S3. Water Contact angle (WCA) of **1′@CF$_3$@melamine** after emulsion separation experiments.

Emulsion types	WCA (°)
Water/Toluene	144 ± 1.1
Water/$CHCl_3$	143 ± 1.3
Water/Gasoline	146 ± 1.0
Water/Kerosene	143 ± 1.4

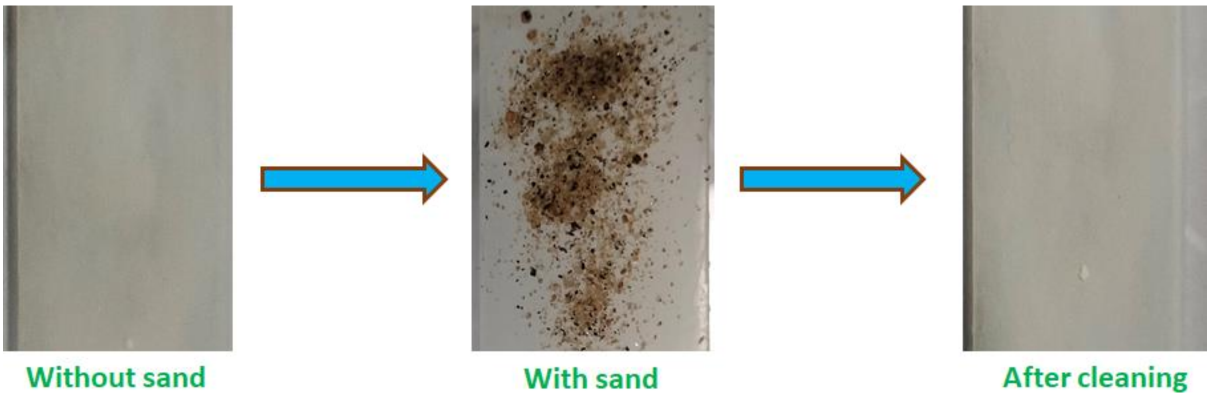

Figure S37. Digital image of **polymer@1′@CF$_3$** glass slide displaying self-cleaning nature.

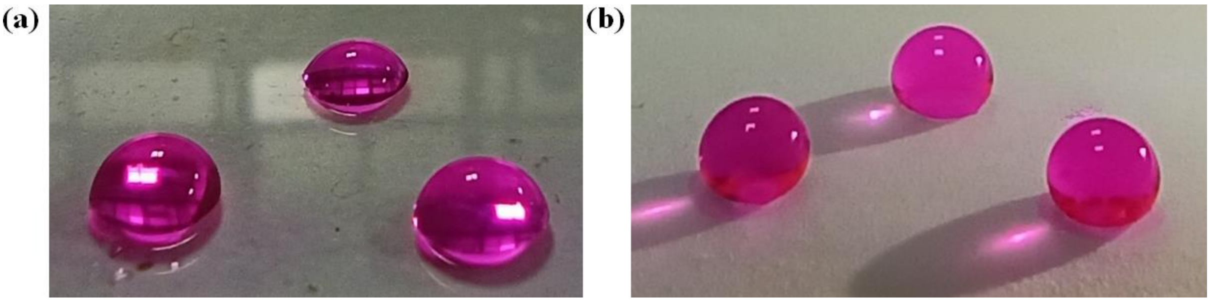

Figure S38. Digital imiages of water droplet on (a) only polymer coated glass and (b) **polymer@1′@CF$_3$** coated glass.

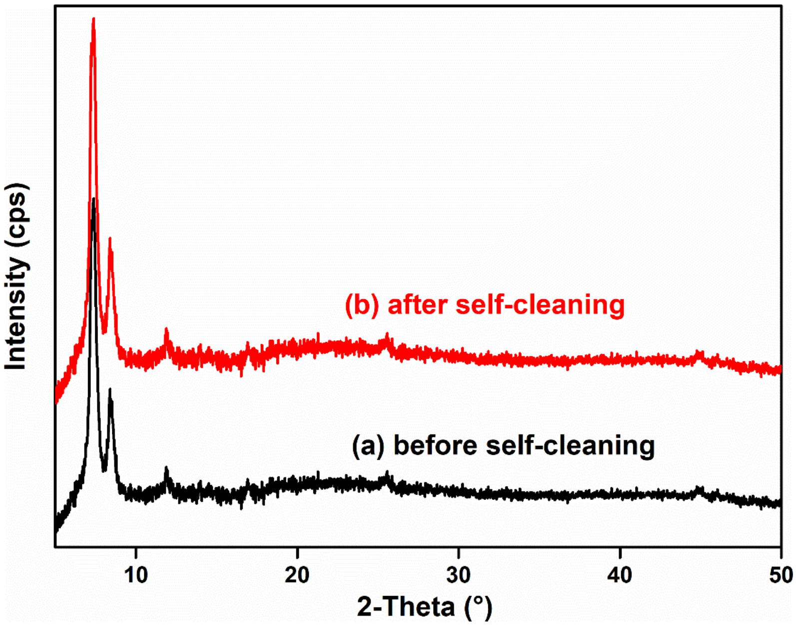

Figure S39. PXRD patterns of polymer@**1′@CF$_3$** coated glass (a) before and (b) after self-cleaning.

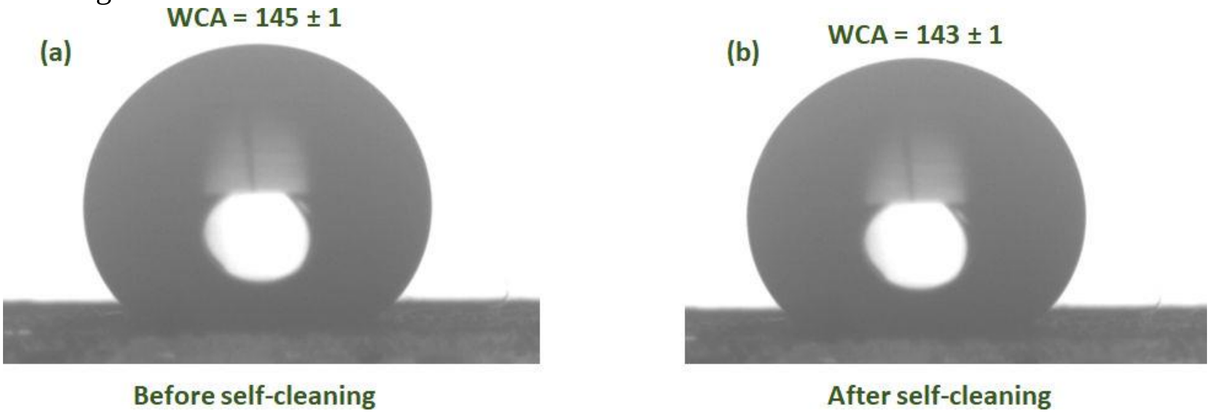

Figure S40. Digital imiages of contact angle of a water droplet on (a) water contact angle of polymer@**1′@CF$_3$** coated glass before self cleaning and (b) polymer@**1′@CF$_3$** coated glass after self-cleaning.

Figure S41. Digital images of **1′@CF$_3$@melamine** composite displaying self-cleaning nature.

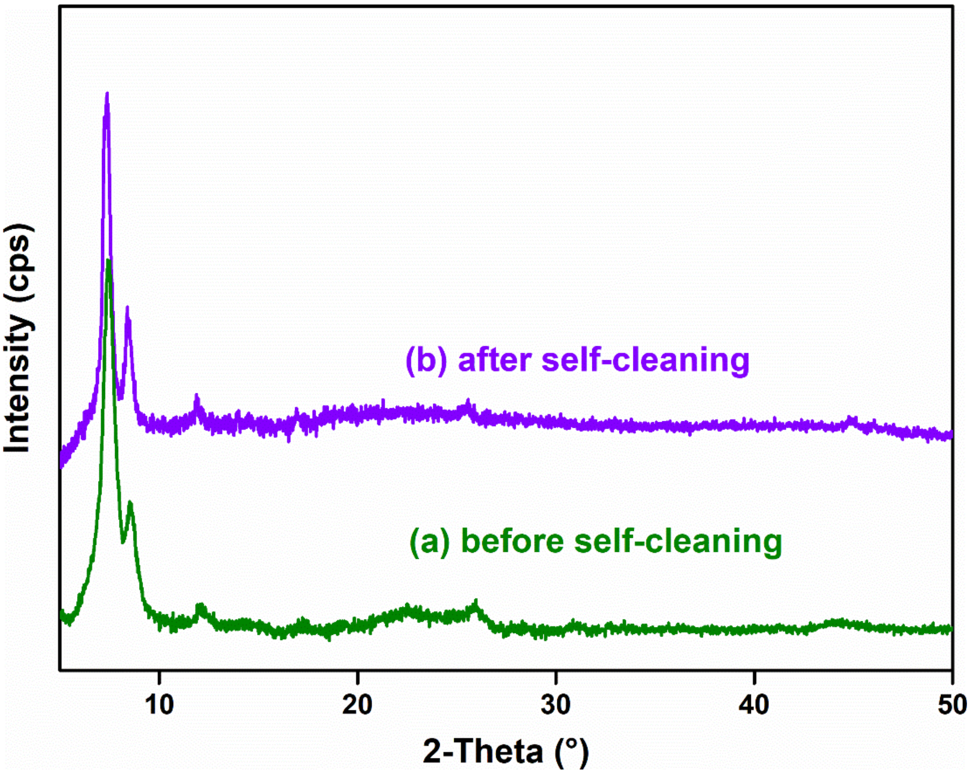

Figure S42. PXRD patterns of **1′@CF$_3$@melamine** composite (a) before and (b) after self-cleaning.

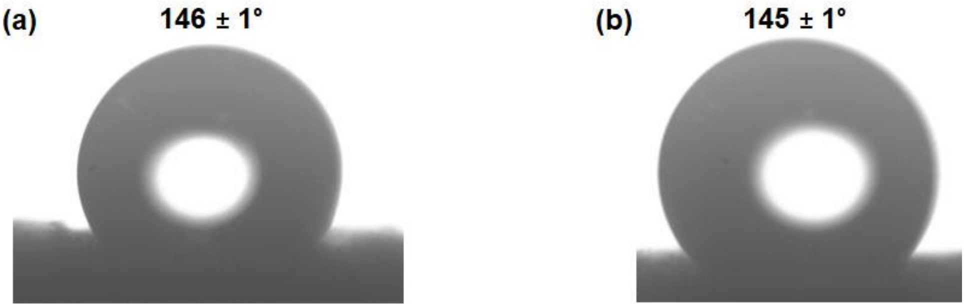

Figure S43. Digital imiages of contact angle of a water droplet on **1′@CF$_3$@melamine** composite (a) before and (b) after self-cleaning.

Table S4. Unit cell parameters of **1′@CF$_3$** obtained by indexing its PXRD data. The obtained values have been compared with parent UiO-66 MOF.

Compound Name	**1′@CF$_3$**	UiO-66
Crystal System	cubic	cubic
a = b = c (Å)	20.797(3)	20.790(3)
V (Å^3)	8994.6(25)	8985.9(9)

Table S5. Absorption capacities (in g/g) of various absorbents for oil absorption.

S. No.	Absorbents	Type of oil	Absorption capacity (g/g)	Ref.
1	**1′@CF$_3$@melamine** composite	gasoline oil motor oil kerosene	26.1 ± 1.2 27.5 ± 1.8 28 ± 0.80	this work
2	PDMS-TiO_2-PU sponge	diesel oil	14.20	2
3	SH-UiO-66@CFs	motor oil silicone oil gasoline kerosene	45.23 38.06 31.87 29.41	3
4	superhydrophobic/superoleophilic sawdust	crude oil	17.50	4
5	cotton fiber modified via the sol-gel method	diesel oil lubrication oil crude oil	25.61 44.24 57.01	5
6	modified jute fiber via the sol-gel method	crude oil diesel oil lubricatiom oil	7.41 8.48 10.29	6
7	mesoporous silica aerogel	petrol oil diesel oil	19.1 18.6	7
8	ultralight cellulose-based aerogel	pump oil diesel oil	22.60 20.9	8
9	cellulose-based aerogel	crude oil diesel oil lubrication oil silicone oil	77.08 91.82 105.83 89.72	9

References:

1. Himsl, D.; Wallacher, D.; Hartmann, M. Improving the Hydrogen-Adsorption Properties of a Hydroxy-Modified MIL-53(Al) Structural Analogue by Lithium Doping. *Angew. Chem. Int. Ed.* **2009,** 48, 4639-4642.
2. Shuai, Q.; Yang, X.; Luo, Y.; Tang, H.; Luo, X.; Tan, Y.; Ma, M. A superhydrophobic poly(dimethylsiloxane)-TiO_2 coated polyurethane sponge for selective absorption of oil from water. *Mater. Chem. Phys.* **2015,** 162, 94-99.
3. Dalapati, R.; Nandi, S.; Gogoi, C.; Shome, A.; Biswas, S. Metal-organic framework (MOF) derived recyclable, superhydrophobic composite of cotton fabrics for the facile removal of oil spills. *ACS Appl. Mater. Interfaces* **2021,** 13, 8563-8573.
4. Zang, D.; Liu, F.; Zhang, M.; Gao, Z.; Wang, C. Novel superhydrophobic and superoleophilic sawdust as a selective oil sorbent for oil spill cleanup. *Chem. Eng. Res. Des.* **2015,** 102, 34-41.
5. Lv, N.; Wang, X.; Peng, S.; Luo, L.; Zhou, R. Superhydrophobic/superoleophilic cotton-oil absorbent: preparation and its application in oil/ water separation. *RSC Adv.* **2018,** 8, 30257-30264.
6. Lv, N.; Wang, X.; Peng, S.; Zhang, H.; Luo, L. Study of the kinetics and equilibrium of the adsorption of oils onto hydrophobic jute fiber modified via the sol-gel method. *Int. J. Environ. Res. Public Health* **2018,** 15, 969.
7. Zhang, C.; Dai, C.; Zhang, H.; Peng, S.; Wei, X.; Hu, Y. Regeneration of mesoporous silica aerogel for hydrocarbon adsorption and recovery. *Mar. Pollut. Bull.* **2017,** 122, 129-138.
8. Zhang, H.; Li, Y.; Xu, Y.; Lu, Z.; Chen, L.; Huang, L.; Fan, M. Versatile fabrication of a superhydrophobic and ultralight cellulose-based aerogel for oil spillage clean-up. *Phys. Chem. Chem. Phys.* **2016,** 18, 28297-28306.
9. Yin, T.; Zhang, X.; Liu, X.; Wang, C. Resource recovery of Eichhornia crassipes as oil superabsorbent. *Mar. Pollut. Bull.* **2017,** 118, 267-274.